# PACKAGE DESIGN FOR HIGH PRECISION MACHINE VISION SYSTEMS

By

Wai Hwa Fong

---

A Thesis Submitted to the Faculty of the

DEPARTMENT OF MECHANICAL ENGINEERING

In Partial Fulfillment of the Requirements

For the Degree of

MASTER OF SCIENCE

In the Department of Mechanical Engineering

THE UNIVERSITY OF MICHIGAN

2 0 0 7

Committee Members:

Albert Shih
Professor

Dragan Djurdjanovic
Assistant Research Scientist and Adjunct Lecturer

# ACKNOWLEDGEMENTS

*For loan of equipment:*
Mr. Dwight Carlson
Chief Executive Officer, Coherix Inc.

Mr. Hollis McNully
General Manager, Semiconducter Business, Coherix Inc.

Ms. Alice Grisham
Human Resources, Coherix Inc.

Mr. Rick Barnich
Coherix Inc.

Dr. Jaspreet Dhupia
Engineering Research Center, University of Michigan

*For technical advice:*
Dr. Deqing Mei
Visiting Scholar, S.M. Wu Manufacturing and Research Center, University of Michigan
Associate Professor, Zhejiang University

*For administrative help and technical advice:*
Dr. Albert Shih
Professor, College of Engineering, University of Michigan

Finally, special thanks to my parents for their financial and morale support.

# TABLE OF CONTENTS

# LIST OF FIGURES

# LIST OF TABLES

# ABSTRACT

High-precision vision systems are optical inspection systems that measure to a few microns. Their mechanical stability is highly sensitive and susceptible to influences from factors such as shock loading, thermal expansion and contraction. Mechanical stability is defined as the resistance to damage or the influence of shock loading particularly during transportation. This study explores the effects of shock loading on the shipping case containing the high-precision vision system, and the robustness of it against such shock. A new package layout is presented. The methodology for the design was developed from literature review and experiments. The shock loading experienced by the case and the machine is investigated by a series of drop tests. The extra 12 mm layer of foam that was added in the final design helped to reduce the acceleration of the vision system in the z-direction by at least 34.9 %. The results were validated by experiments. The new package design of 100 mm thickness in the x-direction, 84 mm of thickness in the y-direction, and 69 mm of thickness in the z-direction, helped to keep the acceleration experienced by the vision system below the benchmark of $50g$ $ms^{-2}$ which is the maximum acceleration that the high-precision vision system can experience without suffering potential damage to the cameras. The new design also maximizes the current material available without adding extra costs.

# CHAPTER 1

# INTRODUCTION

Machine vision is the application of computer vision to the industry and manufacturing. One of the most common applications is the inspection of manufactured goods such as semiconductor chips, automobiles, food and pharmaceuticals. This proves most successful in the controlled environment of the factory floor, offering some important advantages over human vision in terms of cost, speed, precision [1]. However, such systems are highly sensitive to shock and vibrations.

Each high-precision vision system consists of delicate equipment such as cameras, mirrors, and sensitive electronic components. The shipping containers used are typically of high quality, and are sturdy, robust, and waterproof. This reduces the likelihood but does not prevent breakage or misaligned cameras during the shipping process due to rough handling. Foam cushioning material would need to be used to reduce the effects of shock to an acceptable level.

## 1.1. Problem Statement

Machine vision relies heavily on repeatability and precision on the scale of microns. However, due to factors such shock loading and thermal distortion, alignment of cameras may be thrown off.  Insufficient cushioning in packaging containers may cause damage to the cameras as well. The effects of shock loading will need to be studied.

Consider a pair of cameras mounted onto a common plate 30.5 cm (1 ft)

apart. They are then aimed at the same common spot 30.5 cm (1 ft) below. This provides a convenient 45 degree “aiming” angle.

The objectives are to prevent potential damage to the cameras and hold the camera alignment to the original position established during calibration. The accuracy of the camera overlap (looking at the same spot) is not important. Thermal distortion, shock loading, and device mounting techniques need to be considered. The stacking errors from bolted connections are an additional complexity as well. This involves connecting the cameras to the plate (providing some amount of adjustment) and the plate to a vertical structure using bolts.

In this study, the 3DX$^{TM}$ high-precision vision system manufactured by Coherix Inc. will be used.

Valuable time can be saved, if the packaging can be designed such that recalibration of the system is not needed, due to reduced shock loading. Reducing the weight of the system without affecting the robustness and strength of the materials of the machine makes shipping costs to be less expensive. This will in turn help the company reduce costs.

By using a shipping container that has adequate cushioning, breakages can be prevented. As the high-precision vision system is an expensive machine, a breakage can be costly to both the manufacturer and customer.

This research aims to further explore the possibilities of controlling any potential damage to the cameras of the system.

### 1.2. General Overview of the Test Machine

A design already exists for the high-precision vision system and this product is currently being shipped to customers. On going design changes are being considered. Information on designs of similar vision system products by companies are mostly kept confidential, as this market is highly competitive.

The high-precision vision system can inspect on the fly, which means there is no stopping required. Semiconductor parts can move continuously to be inspected and this saves precious time.

Three Opteon 4-Megapixel cameras are installed inside the machine, and this has a 50mm x 50mm field of view. The cameras are mounted at an angle on brackets, with a lighting system installed underneath, at the base of the machine. The cameras capture images of the inspected parts, which are then processed by software to determine if the part is defective.

The lighting is located at the base and is exposed. The lights are integrated to the frame that holds the mirrors and cameras. The mirrors are connected to the frame by bolts. The cameras are mounted on brackets of the frame also by bolts. Refer to Figure 1 for a clearer picture of the components.

**(a)**

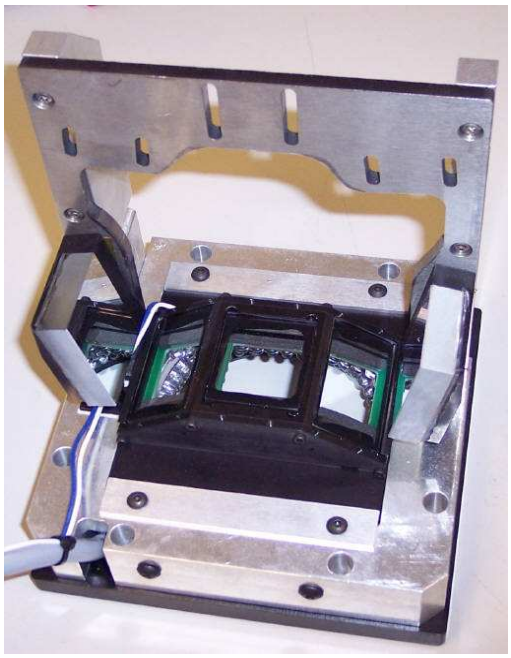

**(b)**

**(c)**


**(d)**

**Figure 1. High-precision vision system main components, (a) outer casing (b) mounting brackets with mirrors (c) lighting system and (d) cameras**

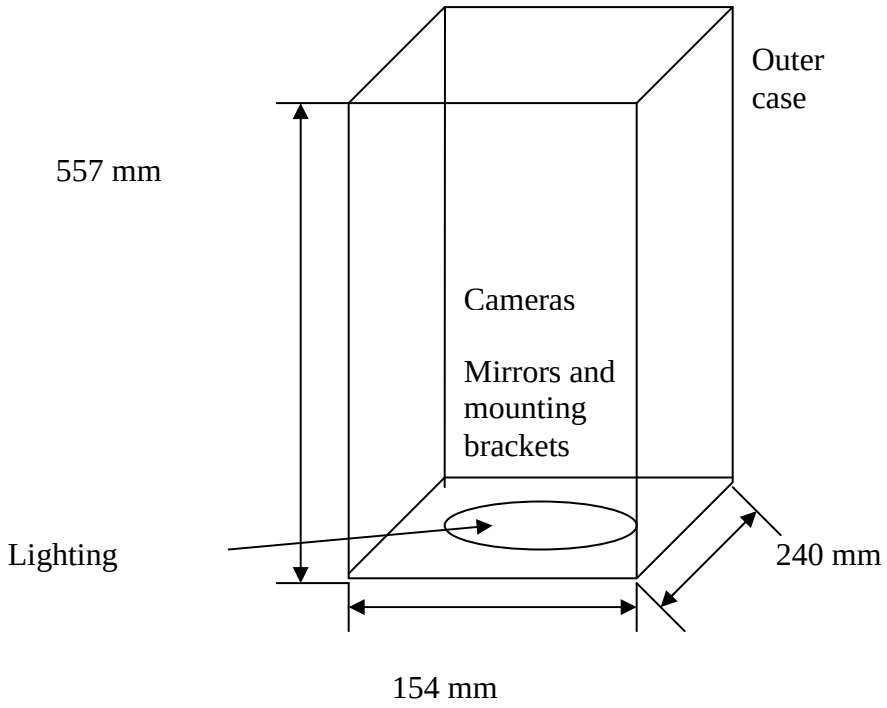


**Figure 2. Locations of main components of high-precision vision system**

### 1.3. Engineering Specifications

The goal is to investigate the effects of shock loading, through the course of this research.

The internal structural parts of the sensor are mainly made up of MIC 6 cast aluminum, and this material is manufactured by Alcoa Mill Products. The Engineering Specifications were developed based on the properties of MIC 6 [2] and the customer requirements.

Also, one major constraint is to work with the current foam materials and shipping case.

| Specification | Quantity/Units |
|---|---|
| Weight of the machine | $\leq$ 15 kg |
| Overall cost of high-precision vision system | $\leq$ $70000 |
| Maximum acceleration | $\leq 50g$ ms$^{-2}$ |

**Table 1. Engineering Specifications**

### 1.4. Prior Research/Literature Review

In the past, there have been systems designed that are inexpensive, have high flexibility for varied inspection tasks, and are easy to integrate onto existing assembly lines [3].

Different systems have different capabilities. Common to them are cameras mounted on a mechanical setup linked to a computer, software to process the images. Changes made to the operating software of the system can drastically improve performance. However, this research will not be focusing on software.

Studies in selecting, designing, analyzing, and using cushions have been done by Mustin [4] for the United States Department of Defense. This was generic and not specific to vision systems. The principles of cushion design will be investigated and applied in the design of the packaging.

A drop test on a container was done by Loh et al. [5] for a camera that was used in a telescope. The camera was found to have survived $50g$ ms$^{-2}$ of acceleration. In this case, the benchmark of $50g$ ms$^{-2}$ will be used when carrying out the research.

The industry leaders in shipping and handling, UPS and Federal Express, have guidelines for shipping fragile electronic equipment [6], [7]. Both recommend a minimum of at least bubble wrap cushioning, foam or packing peanuts with cardboard boxes. However, it is not suitable for fragile electronic equipment.

Fackler and Kutz [8] state that the general rule for protective packaging of electronic equipment is that the product must survive handling, shipping, and storage environments without degradation. Shipping containers for electronic devices must tolerate stacking and handling mechanical devices. Also the packing materials must be chemically inert and not cause detrimental effects of the equipment.

According to Mustin [9], open-cell flexible polyurethane foam is a good packing material and provides optimal cushioning for objects exerting static stresses up to 0.0011 to 0.0034 MPa.

Pelican™ claims that the 1650 model case used in this study is waterproof, crushproof, and dustproof [10]. The hard, rigid shell of the case can tolerate stacking and handling, unlike soft cardboard boxes. Machines have been shipped in the past using Pelican™ 1650 cases without any instances of breakages. The machines arrive at their destination intact, except the cameras are out of alignment. In experimental drop tests that were conducted in the course of this research, the Pelican™ case proved strong and sturdy enough and there were hardly any scratches on the surfaces after the drop. In all the tests, there were also no breakages or cracks on the high-precision vision system machine.

Considering these factors, it can be safely assumed that the Pelican™ case and polyurethane foam prevents breakages. However, due to the layout configuration of the

packing, they do not provide sufficient protection from shock loading that cause the cameras to go out of alignment or suffer potential damage.

According to the EIA-541 standards by the Electronics Industries Association [11], the general requirements for packaging materials is that they must maintain their properties during storage, shipment, distribution, and application.

The ASTM D5276-98 “Standard Test Method for Drop Test of Loaded Containers by Free Fall”, was consulted before the test. This standard is for dropping containers not exceeding 50 kg.

The ASTM D5276-98 standards, include ensuring a correct orientation, accurate control of the drop, lifting devices that do not damage the container, and having an impact surface that is horizontal and flat. Also, the standard says that at three samples should be taken for evaluation. In the conducted drop test, three tests were done in each direction. The standard states that for the test, the container must be packed with the exact contents as if it were going to be shipped [12]. This was done.

The ASTM D6537-00 “Standard Practice for Instrumented Package Shock Testing For Determination of Package Performance” was used as a guide in conducting the drop test. It discusses the apparatus needed, how to do sampling, the test specimen, calibration, conditioning, and procedure. The required apparatus described in the standards were used during the drop test [13].

Most of the procedures in the ASTM D6537-00 were followed.

## 1.5. Research Approach

Initially, a literature search and review was done to gain a better understanding of the topic. The focus was on how shock loading contributed to the mechanical stability.

A shock loading analysis was done to see if vibrations have a significant effect on the stability of the 3DX™.

A redesign of the layout of the package was done. The competence of the design was verified by a series of drop tests.

The goal is not to incur too much additional costs. The present arrangements and materials will be analyzed to see if they can be improved on, trying to maximize the potential of the current materials.

## 1.6. Thesis Outline

Chapter 2 introduces the experimental setup and equipment used to gather data and results. The data acquisition and instrument setup are shown. Procedures are also discussed.

Chapter 3 elaborates on the results from the test to determine the stress-strain curve. Its implementation will be discussed.

Chapter 4 discusses some cushioning and vibrations theory and calculations done.

Chapter 5 discusses parameters selected for the drop test. Results from the drop test and the interpretations of the graphs are also shown.

Chapter 6 explores possible improvements and conclusions, as well as future work.

# CHAPTER 2

# EXPERIMENTAL SETUP

This chapter examines the experimental setup of two types of tests conducted during the course of this research. The tests were a simple compression test to determine the stress-strain relationship of the foam packing material, and a drop test to analyze peak accelerations experienced.

## 2.1. Test for Stress-Strain Curve of Foam

The goal of this test was to get an estimate of the stress-strain relationship for the foam material found in the suitcase, as the manufacturer did not provide any specifications on the foam.

A series of weights were put on top of a block of foam material and the displacement was measured by a set of calipers. To ensure that the pressure distribution was even, a light wooden plank was placed on top of the block of foam material, and the weights in turn placed on top. A Stress-strain curve was then plotted.

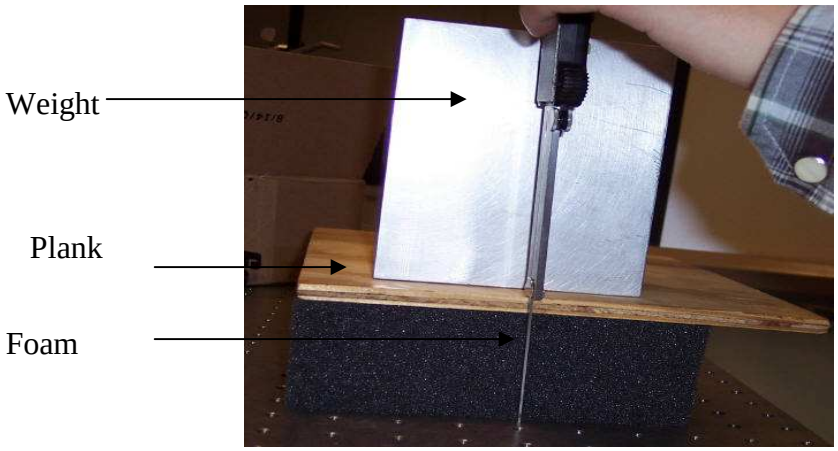


**Figure 3. Experimental setup**

In this experiment, accuracy was not of utmost importance, because only an estimate of the stress-strain relationship was needed. This was so that a starting point could be found and the calculations for the layout of the packing suitcase could proceed. Therefore, this method is justified to determine the stress-strain relationship.

### 2.2. Experimental Setup for Drop Test

The equipment for the experimental setup for the drop test consists of:

| **Equipment** |
|---|
| Accelerometer sensors, PCB® W353 B15/003 |
| Charge amplifier, KIS Type 5010 |
| Analog/Digital converter, National Instruments BNC 2110 |

**Table 2. Electronic equipment for drop test**

The analog/digital converter was connected to the data acquisition card. The charge amplifier was then connected to the analog/digital converter. The accelerometer sensors were then connected to the charge amplifier.

One accelerometer sensor was fixed on the case using super glue. The other was fixed onto the high-precision vision system also using super glue, and slotted through a hole drilled through the case. The accelerometers have a sensitivity value of 10mv/*g*, where g is the acceleration of free fall [14]. The accelerometers were mounted so that its

sensitive axis was aligned as accurately as possible. Also, care was taken to ensure that looseness or loss of contact between the accelerometer and its mounting surface did not happen, in accordance with ASTM D6537-00. Data was collected using LabVIEW® software. The output from the sensors was in terms of voltage (V). The output was scaled down by factors determined by trial and error.

### 2.3. Drop Test Procedure

Following the guidelines, set by the ASTM D6537-00 standards [13], the actual contents and package were used for the test specimen. The initial layout of the machine in the case was exactly the same as that of Figure 4.

**Figure 4. Old layout of case**

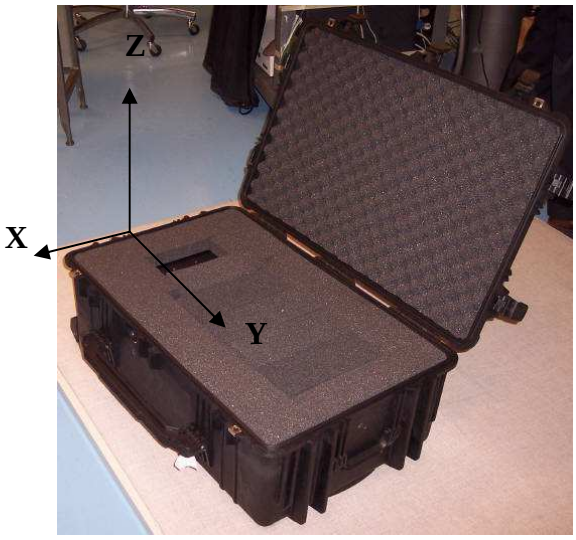


**Figure 5. New layout of case**

It was determined that the layout was inefficient and insufficient at protecting the machine from shock, as the layers of foam at one end were too thin. It was decided to then center the machine in the case so as to optimize the foam packing material. The resultant arrangement is shown in Figure 5.

The shipping case with the high-precision vision system inside of it was dropped from a height of approximately 0.91 m (3 ft) in the x, y, and z-directions as defined in Figure 5.

A trial drop test was made before each actual run to see if the scale values on the amplifier would cause an "overload". If it did, the scale values were adjusted accordingly. The results were logged by LabVIEW®, which then generated a text file with the figures. LabVIEW® was set to capture data over a period of 5 seconds. The figures were then analyzed in excel.

A separate drop test was conducted in the negative z-direction for reasons that will be discussed in a later chapter. For this test, the case was simply flipped over, and the sensors switch around in the opposite direction. The case was the dropped from a height of approximately 0.91 m (3 ft).

Care was taken to ensure that the wires of the two sensors did not touch each other during the drop, as it would have resulted in an "overload" of the amplifier.

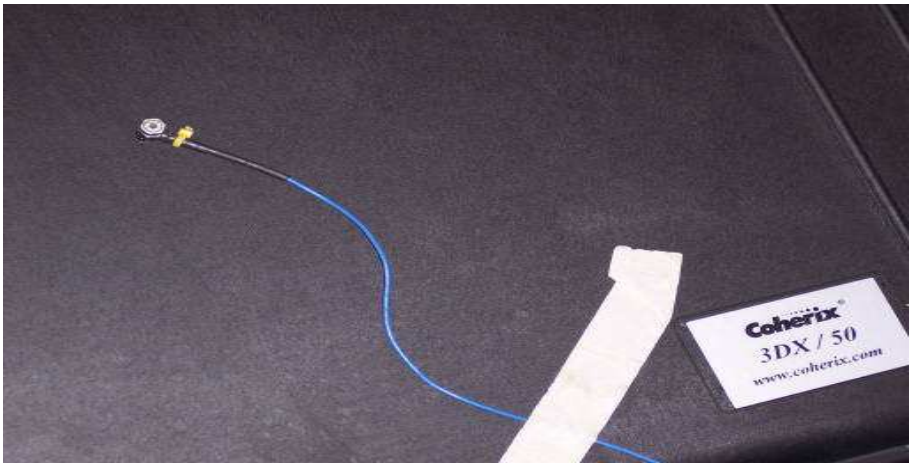


**(c)**

**Figure 6. Accelerometer sensor mounted on case**

In the x, y, and z-directions, the scale factors were 20*g*/V, 50*g*/V, and 30*g*/V respectively. The values of acceleration in terms of *g* were determined by multiplying the outputs with the scale factor.

One of the sensors used during the test is shown in Figure 6. The results of the experiments will be discussed in a later chapter.

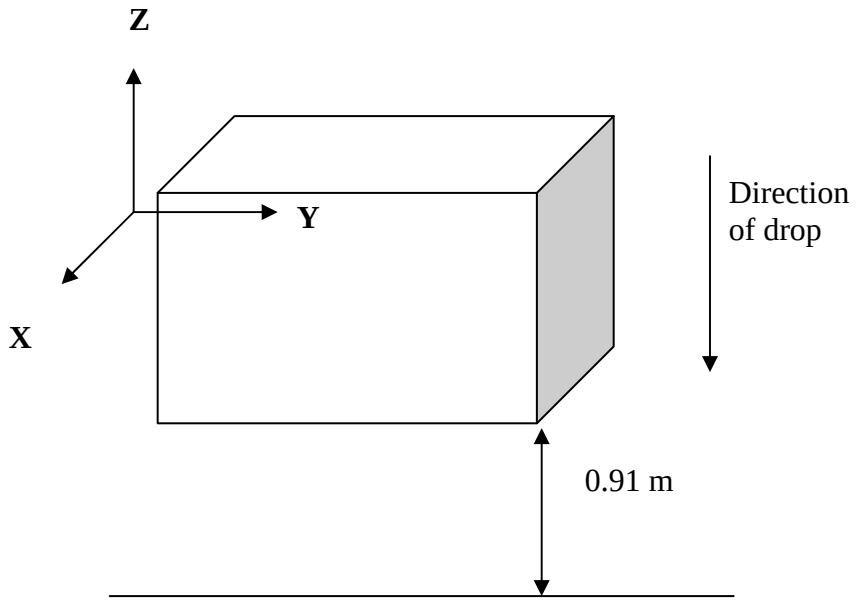


**Figure 7. Direction and height of drop**

# CHAPTER 3

# RESULTS OF FOAM COMPRESSION TEST

In this chapter, the results of the compression test will be discussed. Also, its implementation in calculations, as well as future tests will be examined. An analysis will be done to design a new layout for the case.

## 3.1. Material Properties of Polyurethane Foam

Polyurethane foam was the chosen packaging material. Shuttleworth et al.[15] conducted a comparison of the static and dynamic properties of open-cell flexible polyurethane foam. They plotted a compressive stress versus compressive strain curve as shown in Figure 8.

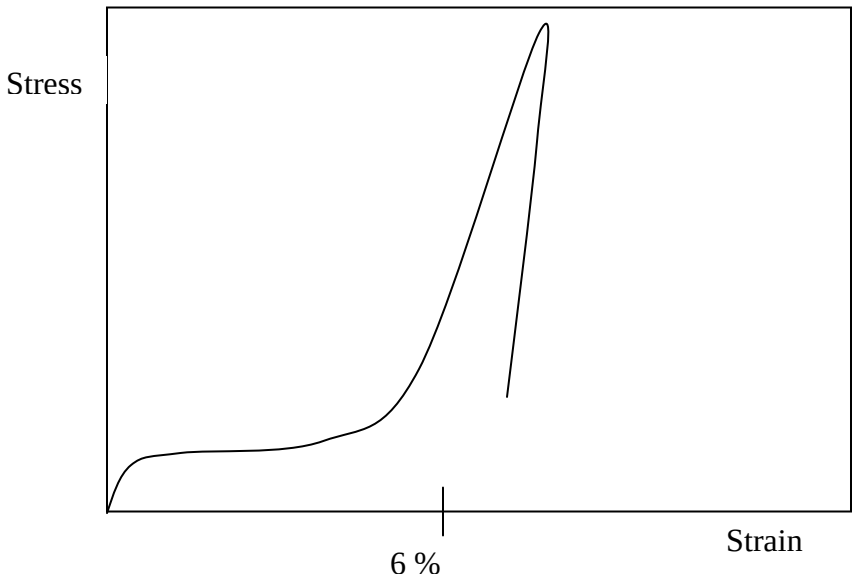


**Figure 8. Approximate shape of compressive stress-strain curve for polyurethane foam [15]**

In the compression test done to verify the stress-strain relationship of the foam, the range of strain was from 0 to 4%. Focusing on the the 4% region of the curve in Figure 8, a similar shape would be expected for the experimental plot from the compression test.

It was found that at 4% strain, the foam material would “buckle” and not give an accurate reading. More sophisticated equipment would need to be used to analyze any further. Elliot et al. [16] conducted a deformation analysis using 3D computed microtomography and managed to analyze up to around 70% strain.

### 3.2. Discussion of Results

Measurements of displacement were taken with total amount of weights at 0, 57.8, 75.6, and 97.9 N. The values of weight were then converted to stress, knowing that the dimensions of the area that the force was applied on was 195 mm by 178 mm. The stress-strain curve of the foam was plotted as shown in Figure 9, using the values of Stress and Strain from Table 4.

| Weight (lbs) | Weight (N) | Stress (MPa) | Displacement (mm) | Strain |
|---|---|---|---|---|
| 0 | 0 | 0 | 0 | 0 |
| 13 | 57.8 | 0.00167 | 0.82 | 0.0144 |
| 17 | 75.6 | 0.00218 | 1.05 | 0.0184 |
| 22 | 97.9 | 0.00282 | 2.01 | 0.0352 |

**Table 3. Data and calculated quantities from compression test**

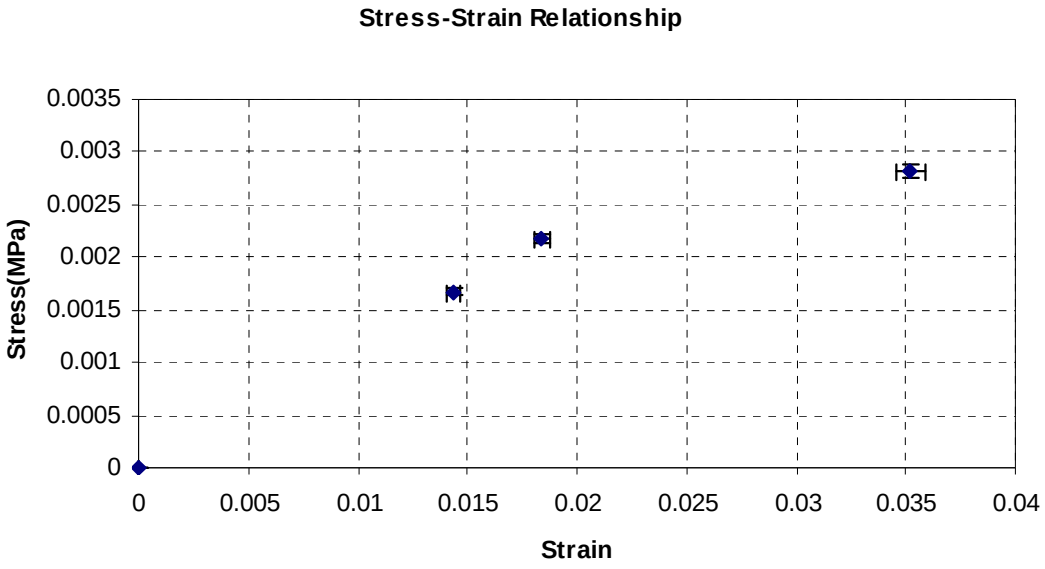


**Figure 9. Stress-strain relationship of open-cell flexible polyurethane foam**

The static stress-strain relationship is needed in order to determine the static deformation of the foam material due to the applied stress from the weight of the machine.

The static deformation gives an expected value of how much the foam will compress. This will give an estimate to see if the new layout, where the machine is centered, will provide adequate cushioning. With this estimate, a drop test can then be performed to measure the accelerations experienced by the machine and the case, and to make a comparison.

The next chapter talks about the calculations and theory to determine the static deformation, and using the result to do a package design.

# CHAPTER 4

# PACKAGE DESIGN

In this chapter, the results from Chapter 3 will be used in calculations for an estimate of static deformation of the foam packing material. The design of the package will be concluded in preparation for the drop test.

## 4.1. Damage Sensitivity

According to Mustin [17], the term “Damage Sensitivity” was coined by Kornhauser. This was a plot of average acceleration against velocity change to give a predetermined displacement to the system. Also, it can be used to predict if damage occurs.

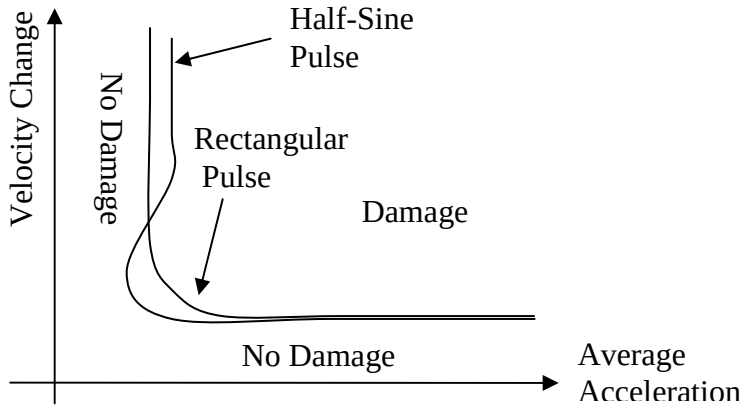


**Figure 10. Kornhauser’s damage-sensitivity curve [17]**

The area to the right of the curves would be the region in which damage might occur. The area to the left would be the region in which damage would not occur. The average acceleration and velocity change of the vision system would be measured by sensors. The velocity change is determined from the area under the curve of the acceleration-time pulse. This model is for objects experiencing continuous pulses of shock or vibration.

The next model would be more suitable for the purposes of this study as it involves only peak accelerations.

### 4.2. Equations of Velocity Shock Isolation

According to Mustin [18], the acceleration of a mass *m* is governed by:

$$\frac{1}{2}mV^2 + A_c T_c [\int_0^{\varepsilon} f(\varepsilon, t) + \psi(t)] = mg(h + T_c \varepsilon) \qquad (1)$$

where t = 0 is taken to be the instant of contact with the floor. $A_c$ is the cushion area, $T_c$ is the cushion thickness, and the value of arbitrary function $\psi(t)$ is determined by the initial boundary conditions. $(1/2)mV^2$ is the instantaneous kinetic energy of *m*, the term containing the integral is the energy stored in the cushion at any instant, and the right-hand member is the potential energy of the mass at its initial height above the instantaneous position. This equation represents the principle of conservation of energy.

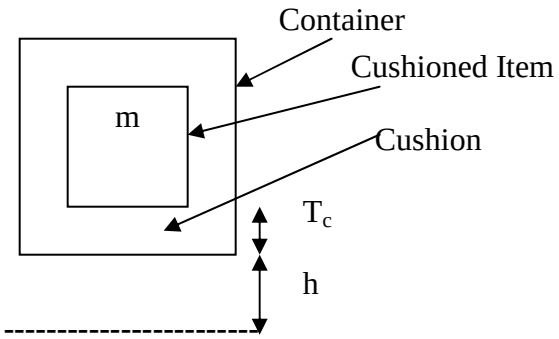


**Figure 11. Cushioning scenario [18]**

For maximum stress when velocity is zero, $\sigma_m$ [19]:

$$\int_0^{\varepsilon_m} f(\varepsilon,t)d\varepsilon + \psi(t) = \frac{mg}{A_c T_c}(h + T_c \varepsilon_m) \tag{2}$$

In the operator notation, where $D^{-1}\sigma_m$ is the energy absorbed per unit volume of cushion [19]:

$$D^{-1}\sigma_m = \sigma_s(\frac{h}{T_c} + \varepsilon_m) \tag{3}$$

The peak force on the machine is equivalent to its inertial force plus its own weight [19]. This is given by the equation:

$$\sigma_m = \sigma_s(G_m + 1) \tag{4}$$

where $G_m$ is the peak acceleration divided by 9.81 $ms^{-2}$. Solving equations (3) and (4), the result is [19]:

$$G_m = \frac{\sigma_m}{D^{-1}\sigma_m}\left(\frac{h}{T_c} + \varepsilon_m\right) - 1 = J\left(\frac{h}{T_c} + \varepsilon_m\right) - 1 \quad (5)$$

Peak acceleration and cushion thickness are now related through the parameter *J*. *J* is known as the cushion factor [19].

In normal situations, h is very much larger than $T_c$ and $\varepsilon_m$ is less than 1.0. Therefore, $G_m$ can be approximated to:

$$G_m = J\frac{h}{T_c} \quad (6)$$

The errors from these simplifications tend to offset one another.

### 4.3. Trial Design of Package

The initially package design was identical to the final design except that the thickness of the cushion at the base of the machine was 57 mm. However, during the series of drop tests, it was found that the accelerations experienced by the high-precision vision system were either close to or exceeded 50*g* $ms^{-2}$.

Equation (6) was used to refine the design. An approximate experimental value of *J* from (6) was found to be 3.401. Therefore, to have an acceleration of 50*g* $ms^{-2}$ or less,

the thickness of the cushion needed to be at least 63 mm. An extra layer of approximately 12 mm of foam was added to bring the thickness to 69mm.

### 4.4. Final Specification of Test Machine and Case

The machine used was exactly the same as the ones that are shipped to customers, except that the cameras were removed. The cameras are delicate and expensive, and as this was an experiment, it was decided not to risk damage to them. However, their weight was negligible as compared to the machine as a whole. This is in accordance with ASTM D6537-00 standards 7.2 [13]. Table 3 lists the specifications measured before the experiment and used in calculations. The shape of the high-precision vision system is approximated to a cuboid.

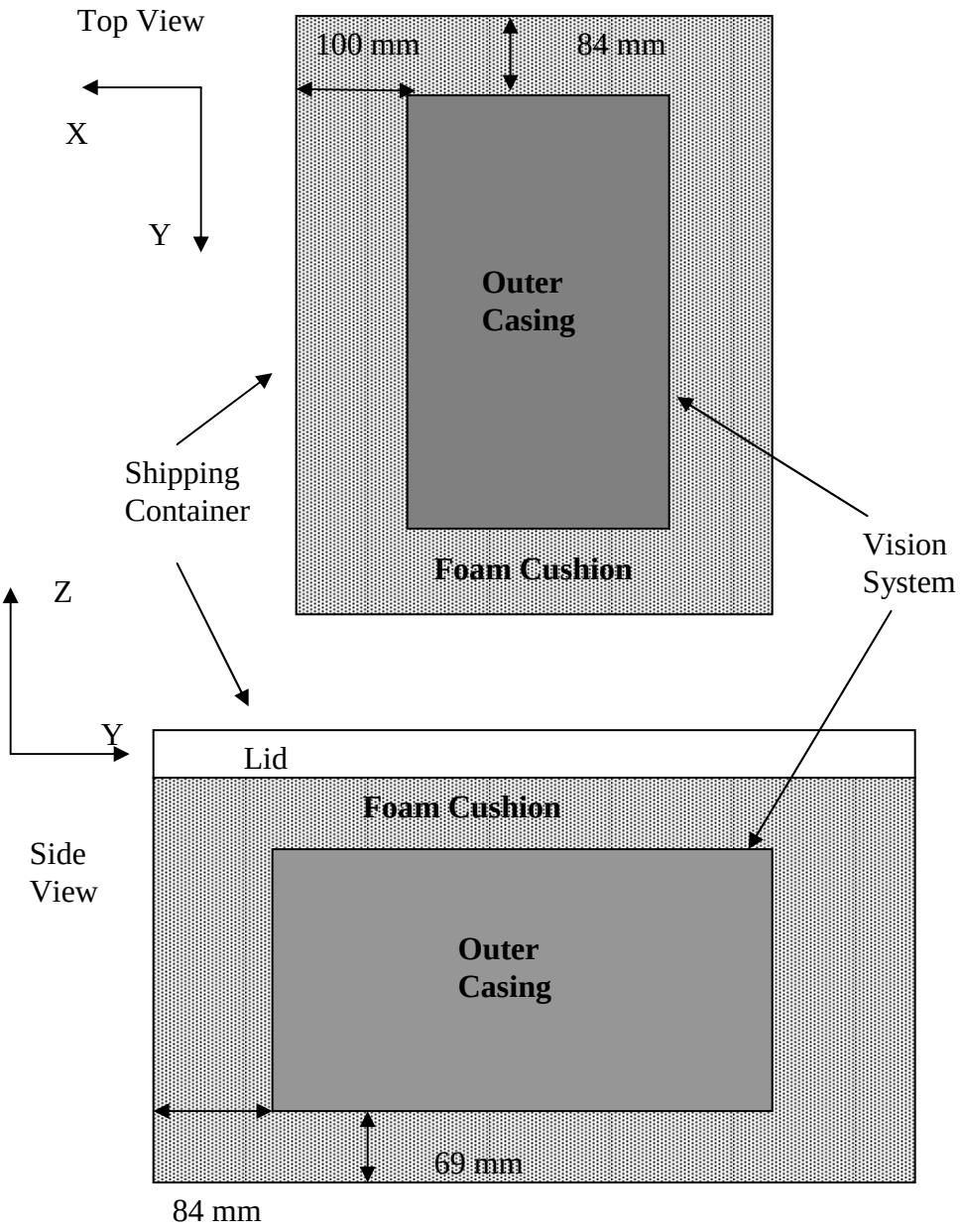


**Figure 12. 2D view of the machine in the case**

| Dimension | Quantity |
|---|---|
| Length of Machine | 557 mm |
| Width of Machine | 240 mm |
| Height of Machine | 154 mm |
| Interior Length of Case | 724 mm |
| Interior Width of Case | 441 mm |
| Interior Height of Case (excluding lid) | 267 mm |
| Weight of Machine | 15 kg |
| Foam Thickness (X) | 100 mm |
| Foam Thickness (Y) | 84 mm |
| Foam Thickness (Z) | 69 mm |

**Table 4. Dimensions of machine and case**

### 4.2. Design of Package

According to Mustin [20], the package design starts by determining the static stress range with the projected area of the object. The ranges of optimum static stresses have to be known in order to narrow down choices. The general shape of the acceleration versus static stress curve is shown in Figure 13 [21].

The lid has convoluted polyurethane foam which reduces impact velocity without compressing large amounts of foam [22].

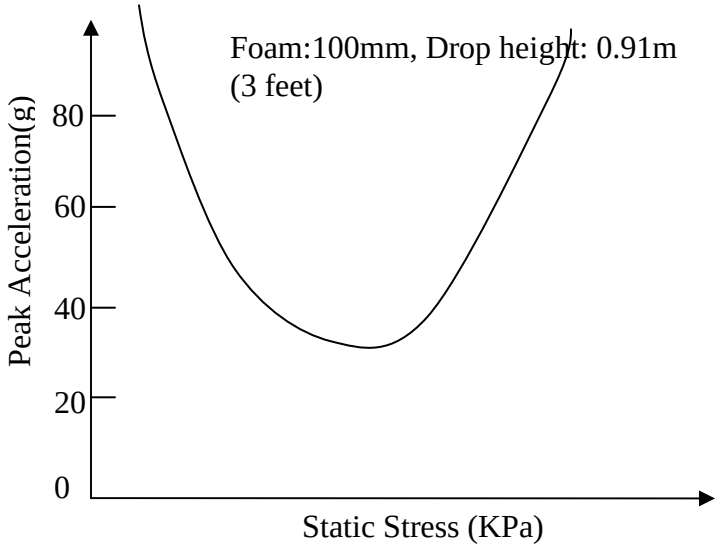


**Figure 13. Acceleration versus static stress [21]**

Knowing that the weight of the machine is approximately 15 kg, the stresses applied by the weight of the machine on the foam can be determined. From there, the static deformation of the foam material can be estimated.

The static stress, $\sigma = \frac{W}{A}$ **,**where A is the cross-sectional area of the face in the plane normal to that of the particular axis. W is the weight of the machine, in this case 15 kg (147 N). ε is the strain of the foam found from the stress-strain curve in Figure 9. Δ is the static deformation of the foam.

| Direction | A ($mm^2$) | σ (MPa) | ε | Δ (mm) |
|---|---|---|---|---|
| X | 85778 | 0.0017 | 0.015 | 1.5 |
| Y | 36960 | 0.004 | 0.1 | 5.71 |
| Z | 133680 | 0.0011 | 0.01 | 0.69 |

.

**Table 5. Calculated parameters**

Theoretically, it was expected that the amplitudes of vibration would be the largest in the y-direction, and therefore having less vibration isolation. However, this was not the case in the drop test. In the test, it was found that the x and y-directions had good vibration isolation. This will be discussed in the next chapter.

# CHAPTER 5

# RESULTS OF DROP TESTS

A series of drop tests were performed using the ASTM D6537-00 standards as a guide. The test specimen contained the actual contents and package except that the cameras were not installed into the machine. The weight of the cameras is negligible as compared to the machine as a whole. This chapter presents and discusses the results of the drop tests. Refer to Figure 5 for the definition of the directions. Acceleration in this case is analogous to the shock experienced.

## 5.1. Plots of the Drop Tests

Using the benchmark of $50g$ $ms^{-2}$, tests on the final design were found to have met this benchmark.

The cushioning layout in both the x and y-directions are almost symmetrical. However, the layout in the z-direction was not symmetrical as the z-direction is normal to the plane of the lid for opening the case.

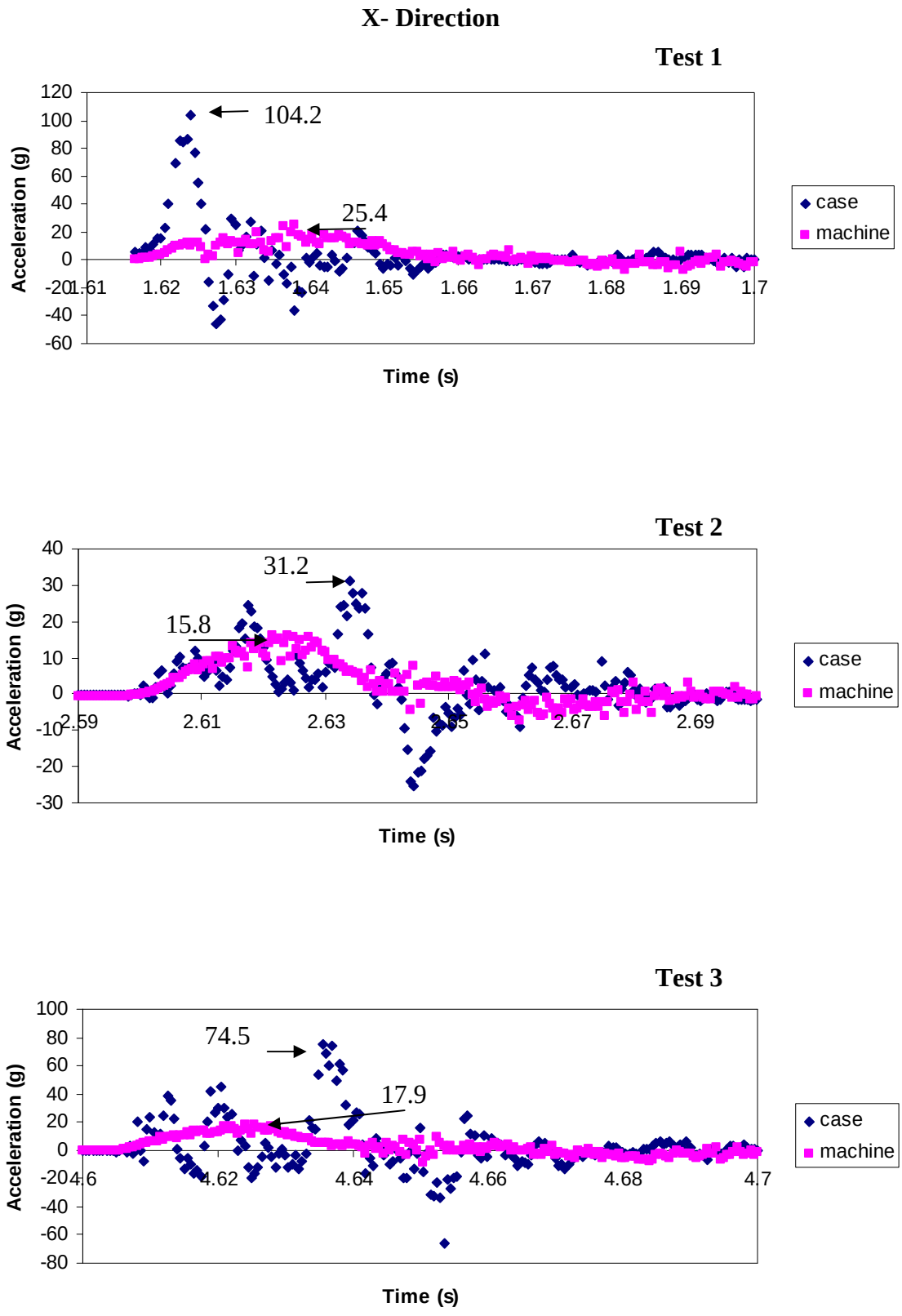


**Figure 14. Acceleration versus time graph in the x-direction**

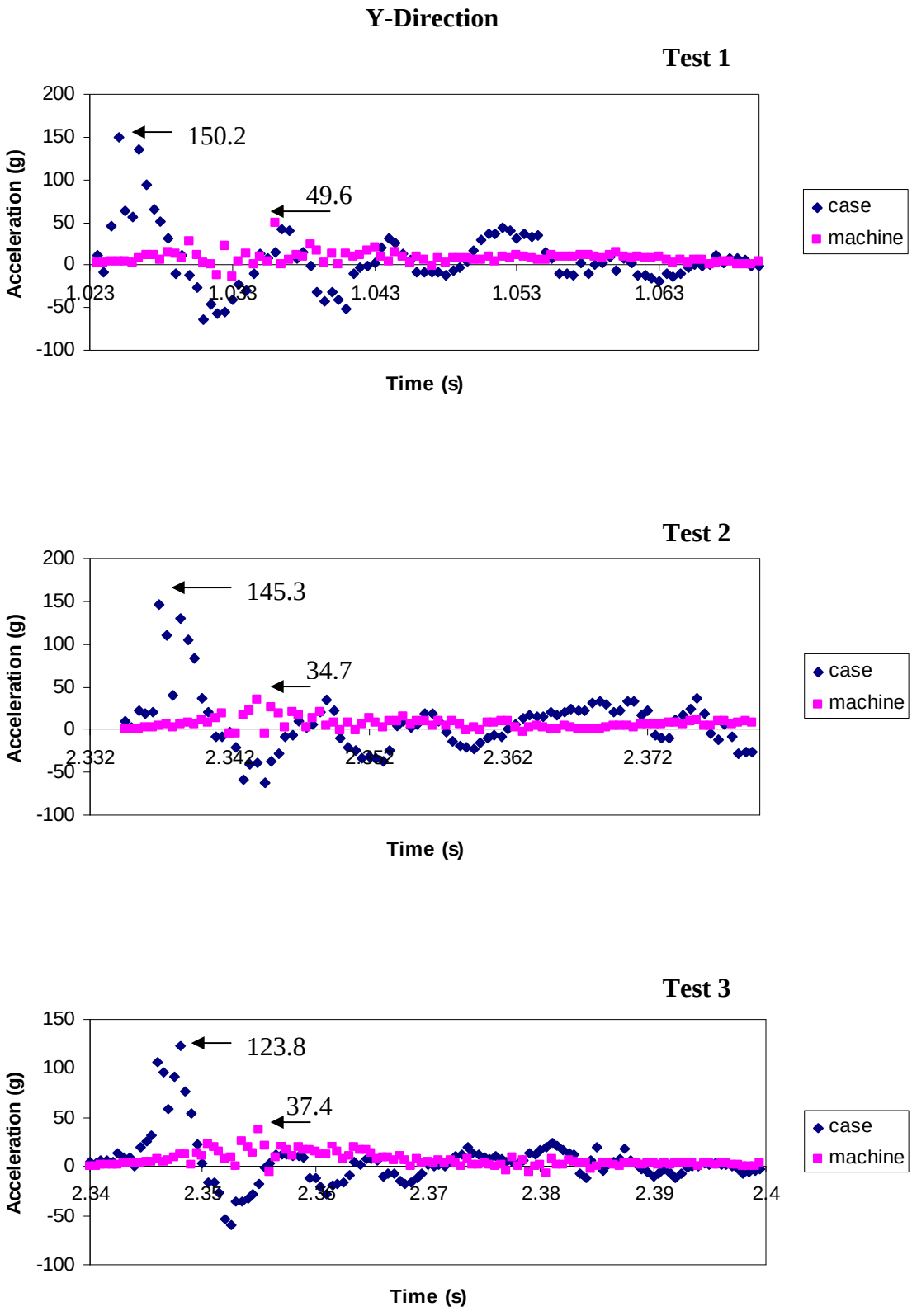


**Figure 15. Acceleration versus time graph in the y-direction**

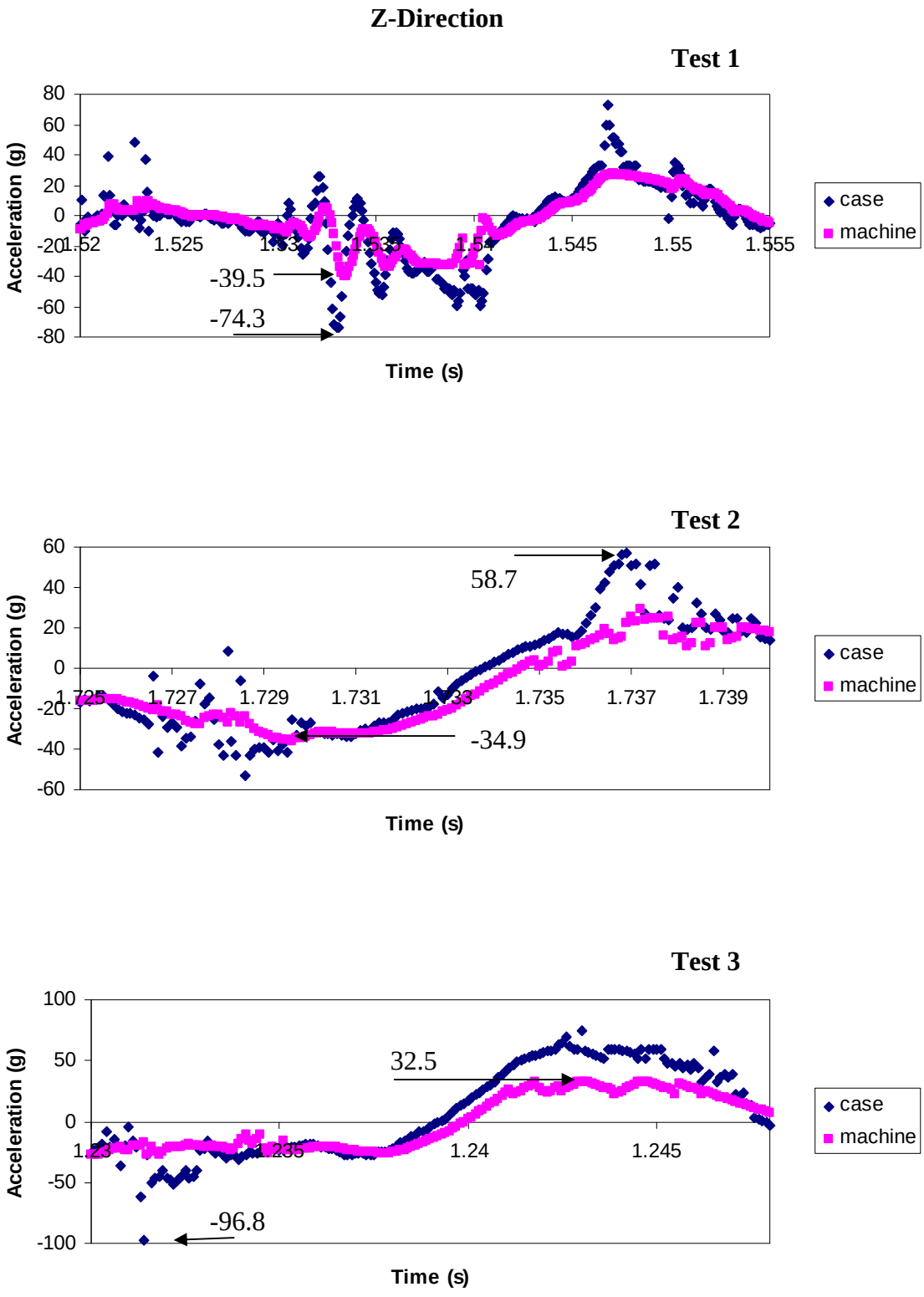


**Figure 16. Acceleration versus time graph in the z-direction**

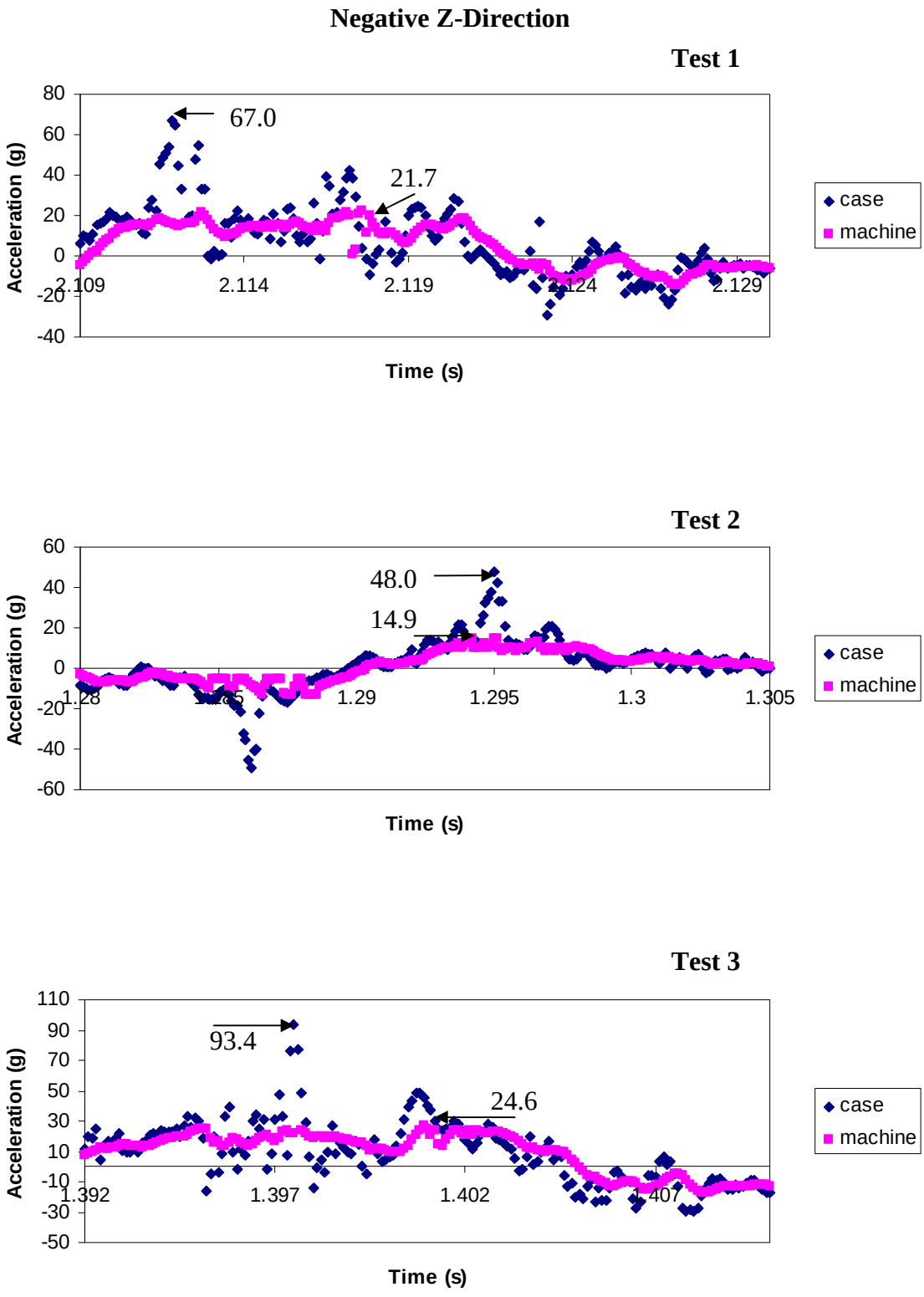


**Figure 17. Acceleration versus Time Graph in the negative z-direction**

It should be noted that the absolute values of the peak accelerations will differ because the drop was done by a person letting go of the case, and not by a machine. It is more important to take note of the differences in peak accelerations of the case and the machine.

In the z-direction of the initial design, the peak acceleration was reduced by only 37% which is not a good figure when compared to the other directions which had a reduction of as much as 300%. The second and third tests of this run, confirms the trend (refer to Appendix A). The acceleration values were 83.2*g*, 68.6*g*, and 129.2*g*. This was well above the benchmark.

A second round of tests was done and this time extra care was taken to position the accelerometers correctly and to ensure the high-precision vision-system was packed tightly. This time 2 out of 3 tests produced a peak acceleration of the high-precision vision system of below the benchmark of 50*g*. The magnitudes of the values were 29.0*g*, 49.5*g*, and 85.2*g*.

It was concluded from these results that the cushioning at the base of the container does not sufficiently protect the machine from shock loading. However, whether or not the cushioning under the lid of the case is sufficient, is inconclusive as the accelerometer could only measure in one direction. So a run of three tests with the container flipped over in the negative z-direction, was carried out. The peak acceleration of the high-precision vision system was found to be well below the 50*g* benchmark. The magnitudes were 20.7*g*, 18.9*g*, and 11.1*g*.

The cushion thickness was then increased from 57 mm to 69 mm and a re-test was done in the z-direction. This time, all the three tests met the benchmark. In the negative z-

direction, due to the decrease of 12 mm of cushion, the acceleration values were higher than the trial design. However, all three tests still were well within the benchmark. The table below showcases the results of the drop test for the final design. As the design in the x and y-directions were unchanged and identical from the trial design, it was assumed that the results would be the same or similar and no further tests were required in those particular directions.

| **Direction** | **Test Number** | | |
|---|---|---|---|
| | 1 | 2 | 3 |
| X | 25.4*g* | 15.8*g* | 17.9*g* |
| Y | 49.6*g* | 34.7*g* | 37.4*g* |
| Z | 39.5*g* | 34.9*g* | 32.5*g* |
| -Z | 21.8*g* | 14.9*g* | 24.6*g* |

**Table 6. Summary of magnitudes of peak accelerations of vision system from final package design**

| **Direction and Test Number** | Z1 | Z2 | Z3 | Average of Z1, Z2, and Z3 | Improvement |
|---|---|---|---|---|---|
| **Trial 1** | 85.2*g* | 68.9*g* | 129.2*g* | 94.4*g* | - |
| **Trial 2** | 49.5*g* | 85.2*g* | 29.5*g* | 54.7*g* | - |
| **Final Design** | 39.5*g* | 34.9*g* | 32.5*g* | 35.6*g* | $\geq$ 34.9 % |

**Table 7. Comparison of accelerations in the z-direction**

For the trial design, the accelerations in the x and y-directions had fulfilled the benchmark, but not that of the z-direction. After refining the design, the average acceleration experienced by the vision system was found to have decreased by 62.3 % from the first trial and 34.9 % from the second trial. In all three tests, the results also fulfilled the benchmark of 50*g* $ms^{-2}$.

# CHAPTER 6

# CONCLUSION AND FUTURE WORK

Ways to control mechanical stability on machine vision systems, more specifically the effects of shock loading, were studied. Damage sensitivity and cushion design literature were consulted. The goal was to apply the principles of cushion design and optimize the currently used container and packaging materials. Compression tests were conducted to determine certain material properties of the polyurethane foam cushion. Drop tests with accelerometers were conducted to investigate how much protection the new package design provided.

This study provided an improved package design with the given constraints. It was recommended to use a 69 mm cushion thickness underneath the high-precision vision system. The thickness in the x-direction would be 100 mm and that of the y-direction, 84 mm. This configuration would protect the high-precision vision system from accelerations of more than $50g$ $ms^{-2}$.

The relationship between the machines natural frequency and the frequency generated in the shipping process should be studied in the future. If they are equal or very close, resonance might occur, causing severe vibration.

# Appendix A

# Graphs of Acceleration against Time from Trial Package Design (Z-Direction and Negative Z-Direction)

## A1. First round of trial tests

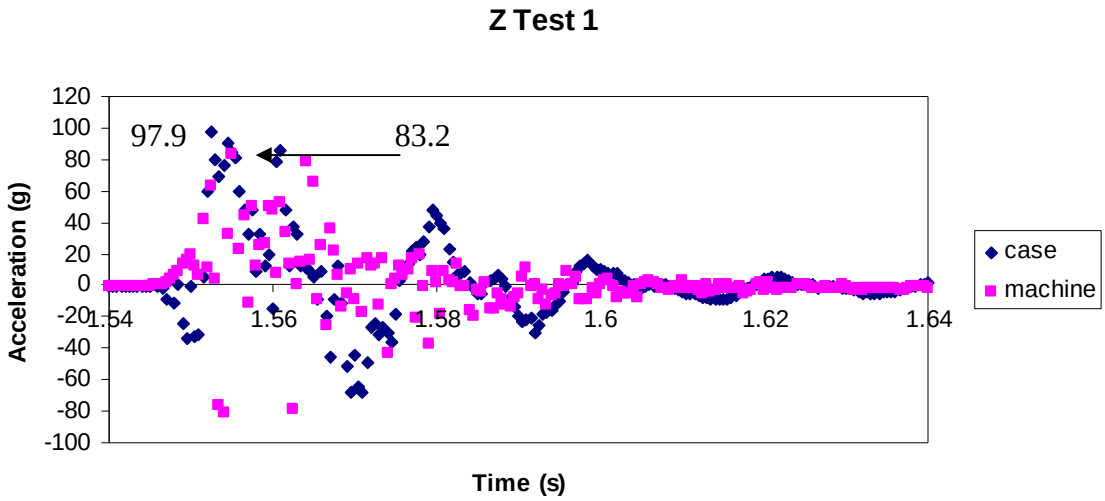


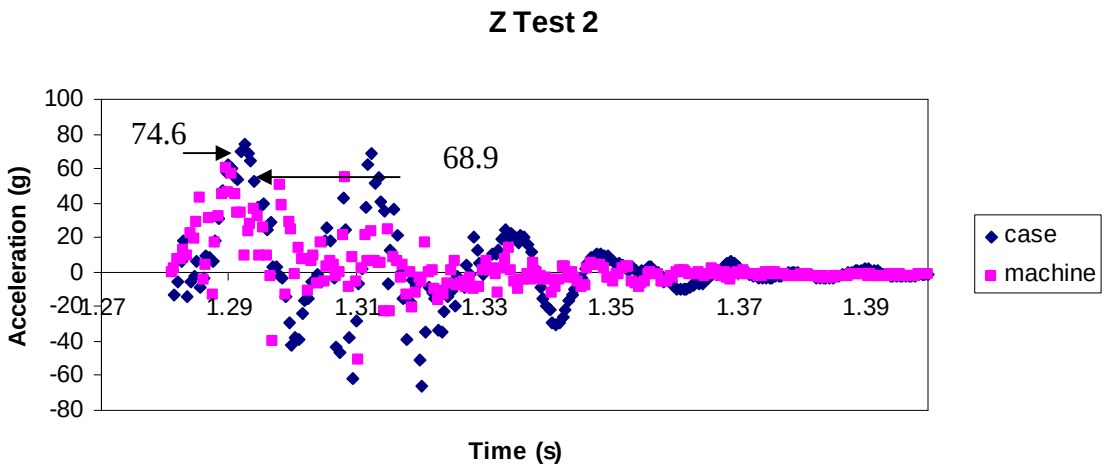

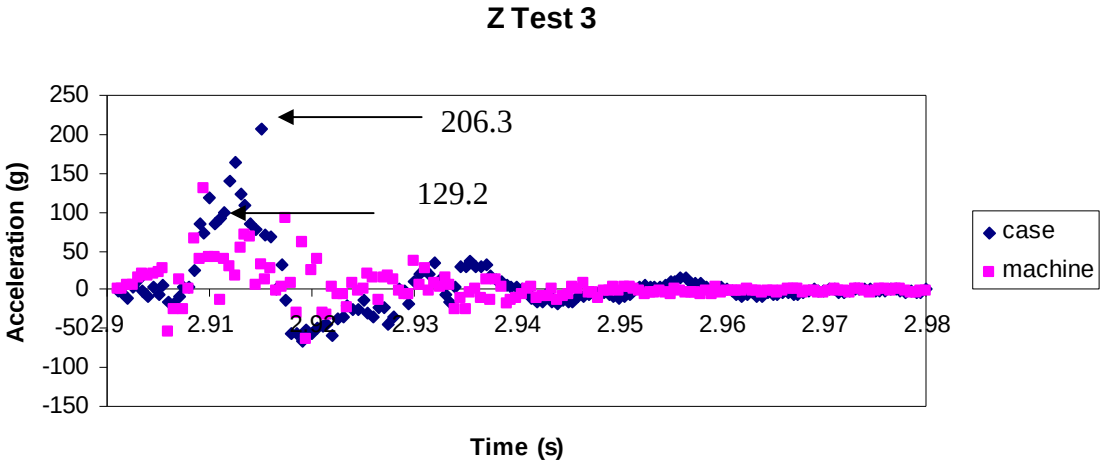


## A2. Second round of trial tests

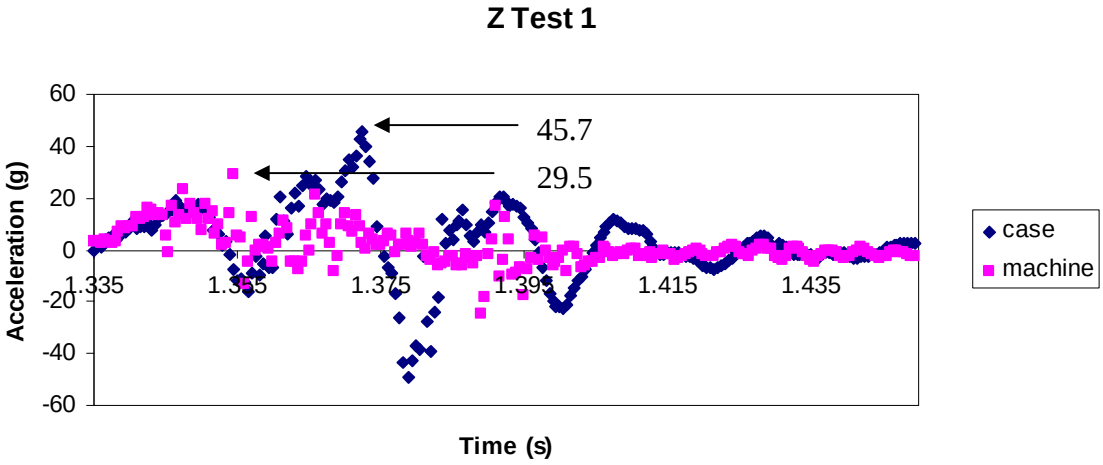

**Z Test 2**

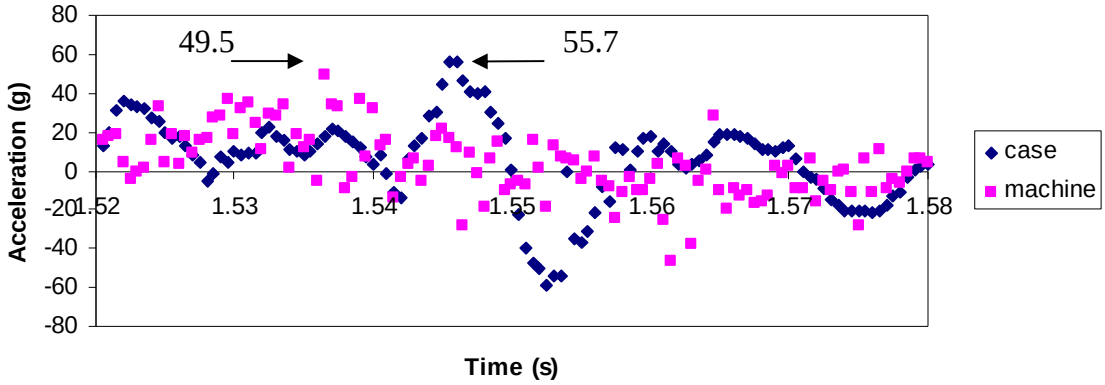


**Z Test 3**

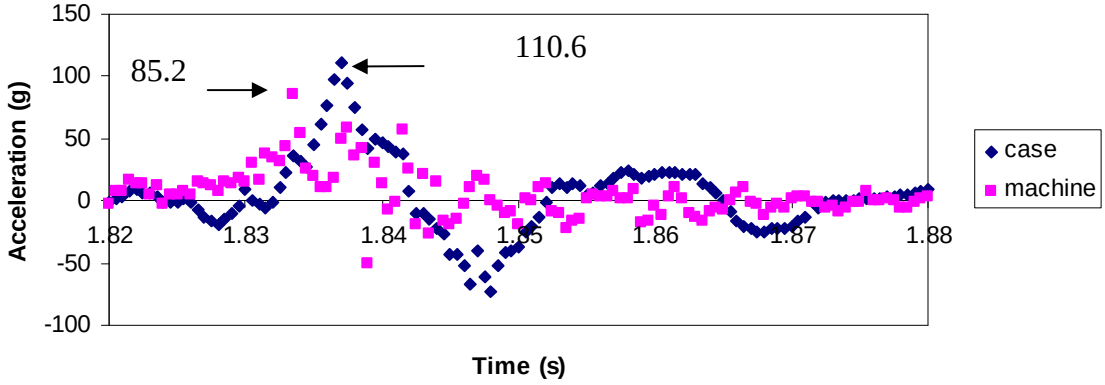


**Negative Z Test 1**

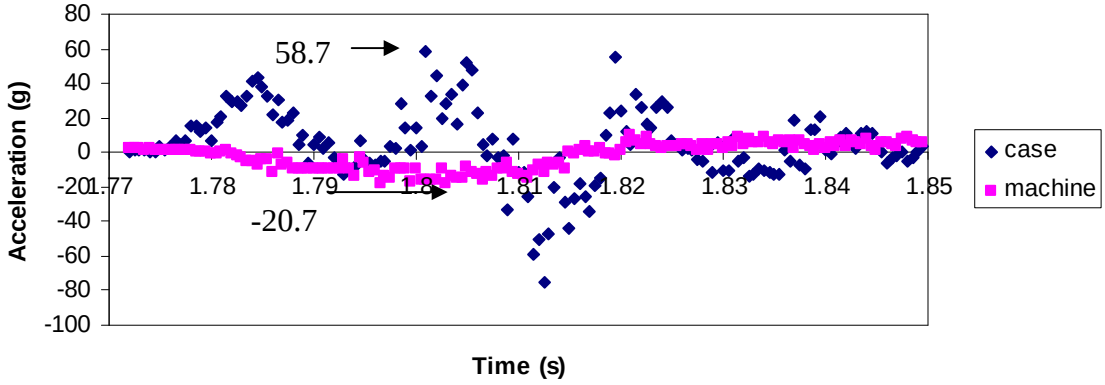

**Negative Z Test 2**

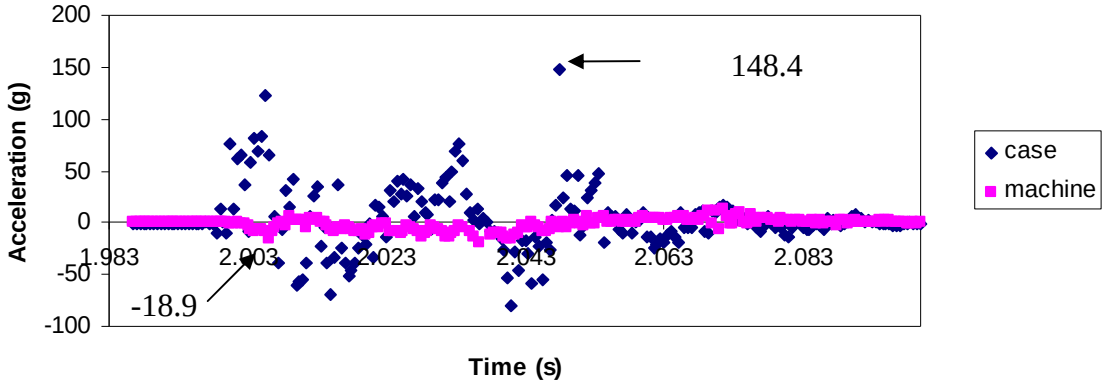


**Negative Z Test 3**

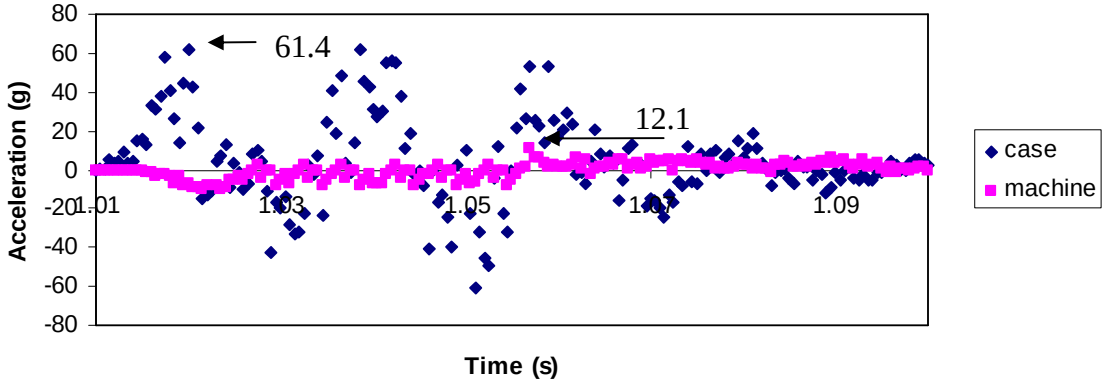

# REFERENCES


1. Francis, Frederick J. (1999). “Wiley Encyclopedia of Food Science and Technology” (2nd Edition) Volumes 1-4. (pp. 1511-1525). John Wiley & Sons.

2. Specifications for MIC6, Alcoa Mill Products-Lancaster Catalog, MIC6 <http://www.alcoa.com/mill_products/catalog/pdf/mic-6.pdf#search=%22properties%20of%20MIC%206%20cast%20aluminium%20%22> retrieved 2007-04-11

3. Gunning, James, Mahon, James, Farrell, Brian, “Flexible Low Cost Machine Vision Inspection systems: A design case study”, SPIE Vol. 2064, 0-8194-1329-1/93

4. Mustins, Gordon S. (1968). “Theory and Practice of Cushion Design”. The Shock and Vibration Information Center United States Department of Defense.

5. Miles P. Loh, Owen Y. Loh, Edwin D. Loh. (2006) “Test of the Shipping Container. Spartan IR Camera for the SOAR Telescope”. Department of Physics and Astronomy. Michigan State University. <http://www.pa.msu.edu/~loh/SpartanIRCamera/ShippingTest.pdf > retrieved on 2007-04-11

6. UPS guidelines for packaging. (1994-2007) United Parcel Service of America, Inc. <http://www.ups.com/content/us/en/resources/prepare/guidelines/index.html?WT.svl=SubNav> retrieved on 2007-04-11

7. Federal Express Guidelines. Pointers on Packaging for Computer Shipments. (2000) FedEx Express Corporation. <http://images.fedex.com/us/services/pdf/PKG_Pointers_Computers.pdf?link=4> retrieved on 2007-04-11

8. Chapter 16, Fackler, Warren C., edited by Kutz, Myer (1998). “Mechanical Engineers' Handbook” (2nd Edition) (pp. 339-352). John Wiley & Sons.

9. Mustins, Gordon S. (1968). “Theory and Practice of Cushion Design”. (pp. 91) The Shock and Vibration Information Center United States Department of Defense.

10. Specifications on Pelican 1650, Online Catalog, Pelican Products Inc. (2007). <http://pelican.com/cases_detail.php?Case=1650> retrieved on 2007-04-11

11. EIA-541. “Packaging Material Standards for ESD Sensitive Items”. Electronic Industries Association

12. “Standard Test Method for Drop Test of Loaded Containers”. ASTM Standards D5276-98 (2004), ASTM International

13. “Standard Practice for Instrumented Package Shock Testing for Determination of Package Performance”. (pp. 2). ASTM Standards D6537-00. ASTM International.

14. Specifications on PCB accelerometer, PCB Specifications Sheet, Piezotronics Vibration Division, Accelerometer, ICP, ECN # 20364 <http://www.pcb.com/spec_sheet.asp?model=353B15&item_id=5115> retrieved on 2007-04-11

15. R. W. Shuttleworth, V. O. Shestopal, P. C. Goss. “Open-cell flexible polyurethane foams: Comparison of static and dynamic compression properties”. Journal of Applied Polymer Science (1985) Volume 30 (pp. 337). 1985 John Wiley & Sons, Inc.

16. J.A. Elliott, A.H. Windle, J.R. Hobdell, G. Eeckhaut, R.J. Oldman, W. Ludwig, E. Boller, P. Cloetens, J. Baruchel. “In-situ deformation of an open-cell flexible polyurethane foam characterised by 3D computed microtomography ”. Journal of Material Science (2002) Volume 37 (pp. 1547).

17. Mustins, Gordon S. (1968). “Theory and Practice of Cushion Design”. (pp. 173) The Shock and Vibration Information Center United States Department of Defense.

18. Mustins, Gordon S. (1968). “Theory and Practice of Cushion Design”. (pp. 64) The Shock and Vibration Information Center United States Department of Defense.

19. Mustins, Gordon S. (1968). “Theory and Practice of Cushion Design”. (pp. 67) The Shock and Vibration Information Center United States Department of Defense.

20. Mustins, Gordon S. (1968). “Theory and Practice of Cushion Design”. (pp. 88-90) The Shock and Vibration Information Center United States Department of Defense.

21. Mustins, Gordon S. (1968). “Theory and Practice of Cushion Design”. (pp. 98) The Shock and Vibration Information Center United States Department of Defense.

22. Burgess, Gary. “Cushioning properties of convoluted foam”. Packaging Technology and Science (1999). Volume 12 (pp. 101). 1999 John Wiley & Sons, Ltd.